Math 415: Modeling hagfish slime

Jean-Luc Thiffeault

(Extracted from *Unraveling hagfish slime* by Chaudhary, Ewoldt, and Thiffeault [3].)

I. INTRODUCTION

Marine organisms present numerous interesting examples of fluid-structure interactions that are necessary for their physiological functions such as feeding [1, 18], motion [2], mechanosensing [15], and defense [16]. A rather remarkable and unusual example of fluid-structure interaction is the production of hagfish slime, also known as hagfish defense gel. The hagfish is an eel-shaped deep-sea creature that produces the slime when it is provoked [7]. Slime is formed from a small amount of biomaterial ejected from the hagfish's slime glands into the surrounding water [9]. The biomaterial expands by a factor of 10,000 (by volume) into a mucus-like cohesive mass, which is hypothesized to choke predators and thus provide defense against attacks (Fig. 1A) [19].

The secreted biomaterial contains thread cells, which possess a remarkable structure wherein a long filament (10–16 cm in length) is efficiently packed in canonical loops into a prolate spheroid (120–150 μm by 50–60 μm) [8, 9], called the skein (Fig. 1B). When mixed with the surrounding water, the fiber (1–3 μm thread diameter) unravels from the skein (Fig. 1C) and forms a fibrous network with other threads and mucous vesicles. This process occurs on timescales of a predator attack (100–400 ms), as apparent from the video evidence [12, 19].

Little is known about mechanisms involved in the rapid thread cell deployment. Motivated by the aforementioned experimental studies, our objective is to investigate the role of viscous hydrodynamics in skein unraveling via a simple physical model.

II. UNRAVELING EXPERIMENT

To motivate the mathematical modeling, we perform a simple experiment demonstrating the force-induced unraveling of thread from a skein. Figure 2 shows the unraveling skein at different time frames. Frame 1 shows the unforced and stable configuration, with no unraveling. Unraveling occurs only when a force is applied from frame 2 onward. There are events when the thread peels away in clumps, but the orderly unraveling recovers quickly. A minimum peeling force seems required to unravel the thread from the skein. A simple estimate of the minimum peeling force based on weak adhesion (van der Waals interaction) between unraveling fiber and skein gives an estimate of 0.1 μN.

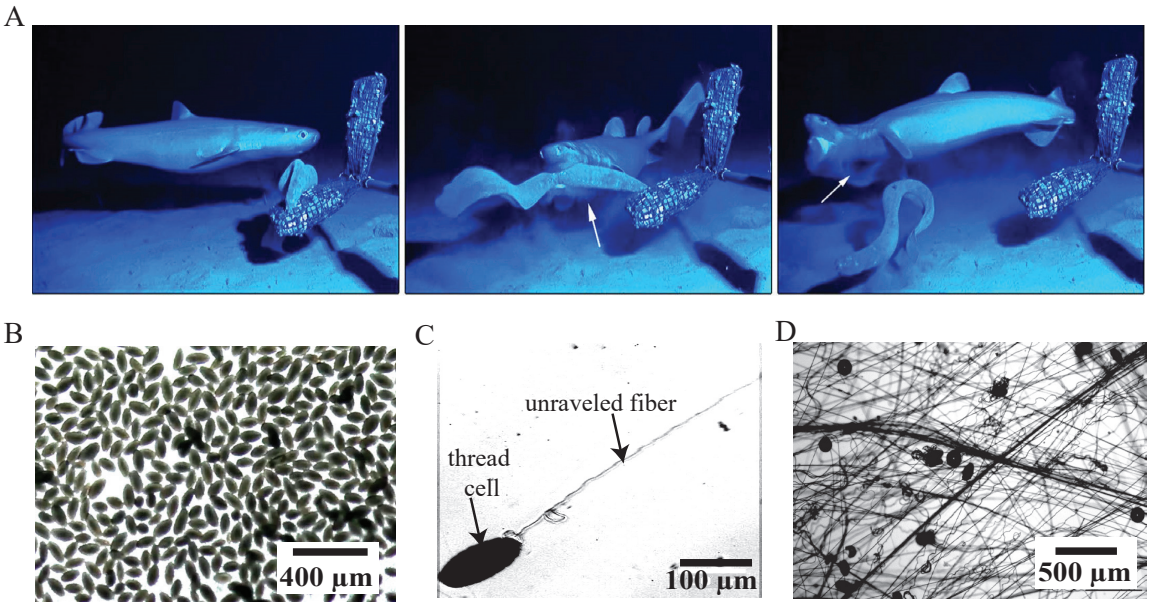

FIG. 1. Slime defends hagfish against predator attacks. (A) Sequence of events during a predator attack (adapted from [19]). On being attacked, the hagfish produces a large quantity of slime that chokes the predator. The process of secretion and slime creation took less than 0.4 s. (B) Slime is formed from the secreted biomaterial, in part containing prolate-shaped thread cells. (C) A thread cell unravels under the hydrodynamic forces from the surrounding flow field and produces a micron-width fiber of length 10–15 cm. (D) The unraveled fibers and mucous vesicles entrain a large volume of water to form a cohesive network.

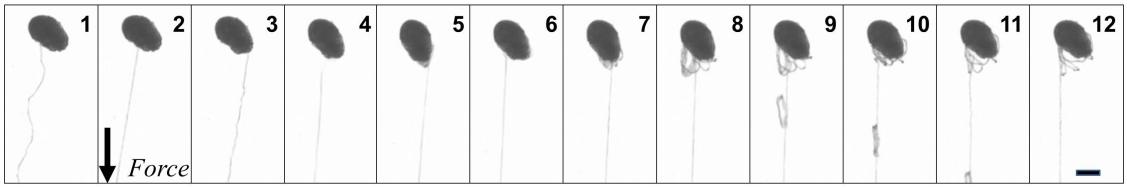

FIG. 2. Unraveling a thread skein by pulling, as viewed with brightfield microscopy. Bottom right scale bar 50 μm.

III. UNRAVELING FROM THE SKEIN

Figure 3 shows a schematic representation of thread unraveling from a skein. The relationship between R and L, respectively the radius of the spherical skein and the length

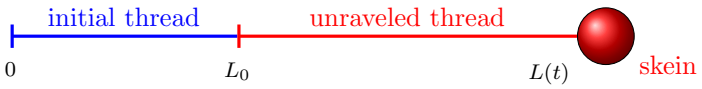

FIG. 3. Simplified model of thread being drawn from a skein. The thread has length $L(t)$ with initial length $L(0) = L_0$. The thread is peeling from the skein at $L(t)$.

of the unraveled thread, is described by volume conservation

$$\frac{d}{dt}\left(\tfrac{4}{3}\pi\eta R^3 + \pi r^2 L\right) = 0 \quad \Longrightarrow \quad \dot{L} = -4\eta R^2 \dot{R}/r^2. \tag{3.1}$$

Here r is the thread radius and $0 < \eta \leq 1$ is the packing fraction of thread into the spherical skein, assumed independent of R. (In this section we keep the packing fraction as a variable, but in all later numerical simulations we take $\eta = 1$, since the skein is fairly tightly packed.) Explicitly, we have

$$R^3 = R_0^3 - \tfrac{3}{4}(L - L_0)r^2/\eta \tag{3.2}$$

with R_0 the initial skein radius and L_0 the initial unraveled length. A convenient way of relating R and L is

$$R = R_0 \left(\frac{L_{\max} - L}{L_{\max} - L_0}\right)^{1/3}, \qquad L_{\max} := L_0 + \tfrac{4}{3}\eta R_0^3/r^2 \tag{3.3}$$

where $L_{\max}$ is the total length of thread that can be extracted and L_0 is the initial unraveled length.

Next, we use a modified form of the work-energy theorem [11] to describe the unraveling dynamics,

$$\dot{E}_{\text{total}} = (T_L - F_{\text{P}}(V))\, V, \qquad V = \dot{L}\,, \tag{3.4}$$

where $\dot{E}_{\text{total}}$ is the rate of change in total energy of the system, T_L is the net force drawing out the thread at a peeling velocity V, and $F_{\text{P}}(V)$ is a velocity-dependent peeling force acting at the peeling site. Neglecting the inertia and changes to the elastic energy of the peeling thread gives

$$T_L = F_{\text{P}}(V), \qquad V = \dot{L}\,. \tag{3.5}$$

A natural dimensionless quantity that will determine the dynamics of the unraveling process is given by the ratio of the net viscous drag force on the thread and the resisting peel force, each of which depends on a characteristic velocity U:

$$\wp := F_{\text{D}}(U)/F_{\text{P}}(U)\,. \tag{3.6}$$

The functional form of the peeling force, $F_{\rm P}(V)$, in general is dependent on parameters such as the chemistry of peeling surfaces, velocity of peeling, etc. In the absence of a known functional form for hagfish thread peeling, we use a simple constitutive form of peeling force that includes a wide range of behavior, given by

$$F_{\rm P}(V) = \alpha V^m, \qquad 0 \le m \le 1, \tag{3.7}$$

for constant $\alpha > 0$ and m. Such a power-law form of peeling force has been observed in several engineered and biological systems [4, 5, 13, 14, 17]. Several other parametric forms of velocity-dependent peeling force exist that are functionally more complex [6, 10]. However, to obtain simple and insightful solutions, we use the power-law form defined above. The form (3.6) allows for the limiting case $m = 0$, a constant peeling force, e.g. to simply counteract van der Waals attractions at the peel site.

For $m > 0$, we can rearrange equation (3.5) for the velocity, $V = \dot{L} = (T_L/\alpha)^{1/m}$. Using (3.1) we can then obtain a solution for the case where the tension at the peeling point, T_L, is constant:

$$\tfrac{4}{3}(R_0^3 - R^3) = (T_L/\alpha)^{1/m}\, r^2 t/\eta\,, \tag{3.8}$$

where $R_0 = R(0)$. From (3.8) we can easily extract the 'depletion time' or 'full-unraveling time' $t_{\rm dep}$ by setting $R = 0$:

$$t_{\rm dep} = \frac{4\eta R_0^3}{3r^2}\,(T_L/\alpha)^{-1/m}\,. \tag{3.9}$$

In the next section we compute this timescale when the thread cells are subjected to different hydrodynamic flow scenarios, which cause different time histories of tension, $T_L(t)$.

IV. FLOW-INDUCED UNRAVELING FROM A PINNED THREAD

Having described the unraveling dynamics in Sec. III for the case of constant tension, T_L, we now consider a thread cell (skein) in a uniform hydrodynamic flow where generally T_L varies in time as the thread-skein geometry changes during unraveling. To simplify the problem, we assume that the thread is pinned at 0 in Fig. 3, with a uniform flow to the right, U. This situation can arise in a controlled experiment if the thread is pinned down, or in the physiological unraveling process if the end of the thread is caught in the network of other threads, or stuck on the mouth of a predator.

The tension in the thread T_L at the peeling point balances the Stokes drag force on the skein of radius R:

$$T_L = 6\pi\mu R\,(U - \dot{L}). \tag{4.1}$$

Using (3.5) and (3.7), we obtain the governing equation for unraveling as

$$(\dot{L})^m = 6\pi\mu\alpha^{-1}R(L)\,(U-\dot{L}). \tag{4.2}$$

From (3.1), since $\dot{L} > 0$ (the thread never 're-spools'), the unspooling speed satisfies $\dot{L} \le U$, i.e. the thread cannot unspool faster than the ambient flow speed. The radius $R(L)$ is given by (3.2).

We nondimensionalize (4.2) using a characteristic length scale R_0 and flow speed U which gives

$$(\dot{L}^*)^m = \wp\, R^*(L^*)\,(1-\dot{L}^*) \tag{4.3}$$

where $\dot{L}^* = \dot{L}/U$ and $R^* = R/R_0$ are the nondimensional unraveling rate and skein radius, respectively. The nondimensional timescale naturally results from these choices as $t^* = t/(R_0/U)$. The dimensionless quantity $\wp$ on the right hand side of (4.3) is given by

$$\wp = \frac{6\pi\mu R_0\, U}{\alpha U^m} = 6\pi\mu R_0\, U^{1-m}\alpha^{-1}\,. \tag{4.4}$$

This is the ratio of characteristic drag to peeling force, as defined in (3.6). If $\wp$ is large (e.g. zero resistance to peeling), then (4.2) implies $\dot{L} \approx U$, that is, in this drag-dominated limit the drag force so easily unravels the skein that it advects with the local flow velocity. In the opposite limit of small $\wp$, we get $\dot{L} \approx 0$ and the skein cannot unravel. Hence, we require $\wp \gg 1$ for a fast unravel time.

To achieve the criterion $\wp \gg 1$, at a flow of speed $U = 1\,\mathrm{m/s}$ and a skein of initial radius $R_0 = 50\,\mu\mathrm{m}$, we require the peeling resistance at this velocity to satisfy $F_\mathrm{P}(1\,\mathrm{m/s}) \ll 1.4\times10^{-6}\,\mathrm{N}$. The estimated van der Waals peeling force is much lower than this threshold, $F_\mathrm{vdW} \sim 10\,\mu\mathrm{N}$. At such a flow speed a skein containing 16.7 cm of thread (an upper bound physiological value) will unravel affinely (kinematically matching the flow speed) in roughly 167 ms. This lower bound estimate is commensurate with the rapidity with which hagfish slime is created (100–400 ms).

In Fig. 4 we show a numerical solution of (4.2) with a uniform flow for some typical physical parameters values, and assuming a moderately-large force ratio $\wp = 10$. (Equation (4.2) is an implicit relation for $\dot{L}$ which must be solved numerically at every time step; it is a Differential-Algebraic Equation rather than a simple ODE [6].) For these parameters, the kinematic lower bound on the depletion time is $L_\mathrm{max}/U \approx 167\,\mathrm{ms}$, and the numerical value is $t_\mathrm{dep} \approx 194\,\mathrm{ms}$.

There is a mathematical oddity where the skein might not get depleted in finite time, depending on the exponent m. To see this, consider a skein close to depletion, $L = L_\mathrm{max} - U\tau$, where $\tau > 0$ is small. The equation for τ is

$$(-\dot{\tau})^m = \wp\left(\frac{U\tau}{L_\mathrm{max}-L_0}\right)^{1/3}(1+\dot{\tau}), \qquad \dot{\tau} < 0. \tag{4.5}$$

Since τ is small and we expect the thread to be drawn out slowly as it is almost exhausted, we take $1 + \dot{\tau} \approx 1$. Hence, we have the approximate form

$$(-\dot{\tau})^m \approx \mathrm{C}^m \, \tau^{1/3}, \qquad \mathrm{C}^m := \wp \, (U/(L_{\max} - L_0))^{1/3} \tag{4.6}$$

for some constant $\mathrm{C} > 0$, with solution

$$\tau(t) \approx \left[\tau_0^{1-\frac{1}{3m}} - \left(1 - \tfrac{1}{3m}\right) \mathrm{C} \, t \right]^{\frac{3m}{3m-1}}. \tag{4.7}$$

The behavior of this solution as the skein is almost depleted depends on m. For $m > 1/3$, the exponent $3m/(3m-1)$ in (4.7) is greater than one, so $\tau(t) \to 0$ as t approaches the depletion time, with $\tau'(t_{\mathrm{dep}}) = 0$ so that $L(t)$ has slope zero when the skein is depleted (as can be seen at the very end in Fig. 4). We can thus rewrite (4.7) as

$$\tau(t) \approx \left[\left(1 - \tfrac{1}{3m}\right) \mathrm{C} \, (t_{\mathrm{dep}} - t) \right]^{\frac{3m}{3m-1}}, \qquad m > 1/3, \quad t \nearrow t_{\mathrm{dep}}. \tag{4.8}$$

For $m < 1/3$, the exponent $3m/(3m-1)$ is negative, but the factor $1 - \frac{1}{3m}$ inside the brackets is also negative, so that $\tau(t)$ asymptotes to zero as $t \to \infty$ and the skein never gets fully depleted. In that case we write (4.7) as

$$\tau(t) \approx \left[\left(\tfrac{1}{3m} - 1\right) \mathrm{C} \, t \right]^{-\frac{3m}{1-3m}}, \qquad m < 1/3, \quad t \to \infty. \tag{4.9}$$

Physically, for $m < 1/3$ the drag force ($\sim \tau^{1/3}$) is decreasing faster than the peeling force ($\sim (\dot{\tau})^m$).

In practice, it is difficult to see the difference between $m \lessgtr 1/3$ numerically. The thread appears to get depleted even for $m < 1/3$ because of limited numerical precision as L approaches $L_{\max}$. The symptom of a problem is that the depletion time starts depending on the numerical resolution for $m < 1/3$. Of course, the skeins in the hagfish slime do not need to get fully depleted to create the gel, so a power $m < 1/3$ is still applicable. When comparing the different flow scenarios we will explore a range of m and define an "effective deployment" time $t_{\mathrm{dep},50\%}$, when 50% of the thread length is unraveled.

REFERENCES

[1] K. L. Bishop, P. C. Wainwright, and R. Holzman. Anterior-to-posterior wave of buccal expansion in suction feeding fishes is critical for optimizing fluid flow velocity profile. *Journal of The Royal Society Interface*, 5(28):1309–1316, Jun 2008.

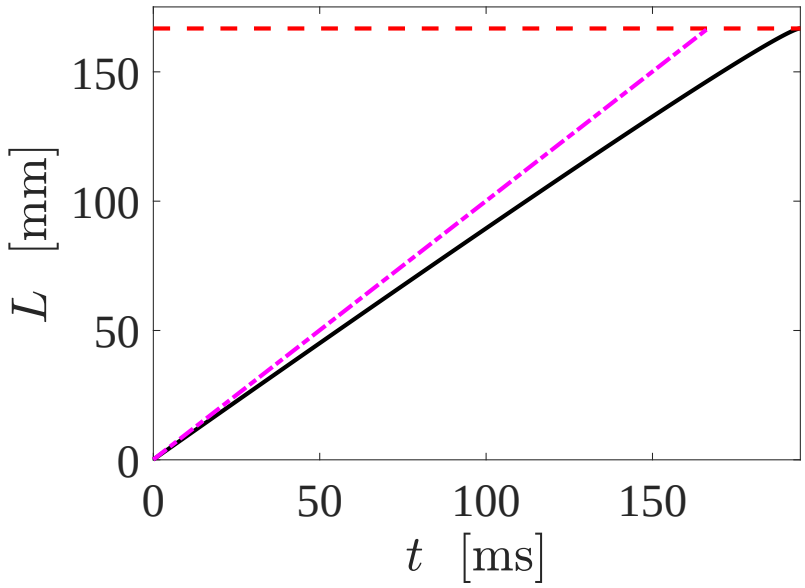

FIG. 4. Numerical solution (solid line) of (4.2) for the parameter values $R_0 = 50\,\mu$m, $L_0 = 2R_0$, $\wp = 10$, $m = 1/2$, $U = 1\,$m/s. The $-$ — line is the upper bound $L = L_0 + Ut$. The horizontal dashed line is at $L = L_{\max}$, when the skein is fully unraveled. Even for such a moderate force ratio $\wp = 10$ the thread unravels almost as fast as the upper bound.

[2] J. W. Chapman, R. H. G. Klaassen, V. A. Drake, S. Fossette, G. C. Hays, J. D. Metcalfe, A. M. Reynolds, D. R. Reynolds, and T. Alerstam. Animal orientation strategies for movement in flows. *Current Biology*, 21(20):R861–R870, 2011.

[3] G. Chaudhary, R. H. Ewoldt, and J.-L. Thiffeault. Unraveling hagfish slime, 2018. Preprint.

[4] P.-P. Cortet, M. Ciccotti, and L. Vanel. Imaging the stick-slip peeling of an adhesive tape under a constant load. *Journal of Statistical Mechanics*, 2007:P03005, Mar. 2007.

[5] M.-J. Dalbe, S. Santucci, P.-P. Cortet, and L. Vanel. Strong dynamical effects during stick-slip adhesive peeling. *Soft Matter*, 10(1):132–138, 2014.

[6] R. De, A. Maybhate, and G. Ananthakrishna. Dynamics of stick-slip in peeling of an adhesive tape. *Physical Review E*, 70:046223, 2004.

[7] S. W. Downing, W. L. Salo, R. H. Spitzer, and E. A. Koch. The hagfish slime gland: a model system for studying the biology of mucus. *Science*, 214:1143–1145, 1981.

[8] B. Fernholm. Thread cells from the slime glands of hagfish (myxinidae). *Acta Zoologica*, 62(3):137–145, 1981.

[9] D. S. Fudge, N. Levy, S. Chiu, and J. M. Gosline. Composition, morphology and mechanics of hagfish slime. *Journal of Experimental Biology*, 208:4613–4625, 2005.

[10] M. A. Griffin, A. J. Engler, T. A. Barber, K. E. Healy, H. L. Sweeney, and D. E. Discher. Patterning, prestress, and peeling dynamics of myocytes. *Biophysical Journal*, 86:1209–1222, Feb. 2004.

[11] D. C. Hong and S. Yue. Deterministic chaos in failure dynamics: Dynamics of peeling of

adhesive tape. *Physical Review Letters*, 74(2):254–257, Jan. 1995.
[12] J. Lim, D. S. Fudge, N. Levy, and J. M. Gosline. Hagfish slime ecomechanics: testing the gill-clogging hypothesis. *J. Exp. Biol.*, 209:702–10, 2006.
[13] Z. Liu, H. Lu, Y. Zheng, D. Tao, Y. Meng, and Y. Tian. Transient adhesion in a non-fully detached contact. *Scientific Reports*, 8(1):6147, 2018.
[14] I. K. Mohammed, M. N. Charalambides, and A. J. Kinloch. Modeling the effect of rate and geometry on peeling and tack of pressure-sensitive adhesives. *Journal of Non-Newtonian Fluid Mechanics*, 233:85–94, 2016.
[15] P. Oteiza, I. Odstrcil, G. Lauder, R. Portugues, and F. Engert. A novel mechanism for mechanosensory-based rheotaxis in larval zebrafish. *Nature*, 547(7664):445–448, Dec 2017.
[16] R. J. Waggett and E. J. Buskey. Calanoid copepod escape behavior in response to a visual predator. *Marine Biology*, 150(4):599–607, 2006.
[17] Z. Wang, Z. Wang, Z. Dai, and S. N. Gorb. Bio-inspired adhesive footpad for legged robot climbing under reduced gravity: Multiple toes facilitate stable attachment. *Applied Sciences*, 8(1):114, 2018.
[18] S. Yaniv, D. Elad, and R. Holzman. Suction feeding across fish life stages: flow dynamics from larvae to adults and implications for prey capture. *Journal of Experimental Biology*, 217(20):3748–3757, Apr 2014.
[19] V. Zintzen, C. D. Roberts, M. J. Anderson, A. L. Stewart, C. D. Struthers, and E. S. Harvey. Hagfish slime as a defence mechanism against gill-breathing predators. *Scientific Reports*, 1:131, Oct. 2011.

Appendix A: Matlab code to solve Eq. (4.3)

This code is freely available at `https://github.com/jeanluct/hagfish-unravel`.

```
function [t,L,R] = Lsolve_pinned_thread(m,P,L0,dLmax,unfrac)

% m, P are dimensionless.
% L0, dLmax scaled by R0.
% unfrac is a fraction in (0,1] denoting the unraveled thread fraction at
% which to stop.
if nargin < 5, unfrac = 1; end

R0 = 1;
tmax = inf;

f = @(t,tau) rhs(t,tau,m,P,L0,dLmax,unfrac);
fe = @(t,tau) events(t,tau,m,P,L0,dLmax,unfrac);

opts = odeset('Events',fe,'RelTol',1e-8,'AbsTol',1e-8,'NonNegative',1);

% Solve for tau = Lmax - L.
[t,tau] = ode45(f,[0 tmax],dLmax,opts);
```

```
Lmax = L0 + dLmax;
L = Lmax - tau;
R = R0*nthroot(1 - (L-L0)/dLmax,3);

% ========================================================================
function dtau = rhs(t,tau,m,P,L0,dLmax,unfrac)

Lmax = L0 + dLmax;
L = Lmax - tau;
R = nthroot(1 - (L-L0)/dLmax,3);

if R < 0
  warning('Lsolve_pinned_thread:Rnegative','R=%g < 0 at t=%g.',R,t)
end

f = @(x) (x.^m + P*R*(x - 1));

% The thread equation to solve for x = dL/dt.
dL = fsolve(f,1,optimset('Display','off','TolX',1e-15));

if dL > 1
  warning('Lsolve_pinned_thread:dLabove1','dL/dt=%g > 1 at t=%g.',dL,t)
end

if dL < 0
  warning('Lsolve_pinned_thread:dLnegative','dL/dt=%g < 0 at t=%g.',dL,t)
end

dtau = -dL;

% ========================================================================
function [value,isterm,direc] = events(t,tau,m,P,L0,dLmax,unfrac)

Lmax = L0 + dLmax;
L = Lmax - tau;

value(1) = unfrac - (L-L0)/dLmax;
isterm(1) = 1;
direc(1) = 0;
```